

Fair Weather Neutron Bursts from photonuclear reactions by Extensive Air Shower core interactions in the ground and implications for Terrestrial Gamma-ray Flash signatures

Gregory. S. Bowers¹, Xuan-Min Shao¹, William Blaine¹, Brenda Dings¹, David M. Smith², Jeff Chaffin², John Ortberg², Hamid K. Rassoul³, Cheng Ho¹, Lukas Nellen⁴, Nissim Fraija⁵, C. Alvarez⁶, J.C. Arteaga-Velzquez⁷, V. Baghmany⁸, E. Belmont-Moreno⁹, K.S. Caballero-Mora⁶, A. Carramiana¹⁰, S. Casanova⁸, E. De la Fuente¹¹, M.M. Gonzalez¹², F. Hueyotl-Zahuantitla⁶, O. Martinez¹³, J.A. Matthews¹⁴, E. Moreno¹³, M. Newbold¹⁵, E.G. Prez-Prez¹⁶, I. Torres¹⁰,

¹Los Alamos National Laboratory, Los Alamos, NM, USA

²University of California Santa Cruz, Santa Cruz, CA, USA

³Florida Institute of Technology, Melbourne, FL, USA

⁴Instituto de Ciencias Nucleares, Universidad Nacional Autónoma de México, México D.F., México

⁵Instituto de Astronomía, Universidad Nacional Autónoma de México, México D.F., México

⁶Universidad Autónoma de Chiapas, Tuxtla Gutiérrez, Chiapas, México

⁷Universidad Michoacana de San Nicolás de Hidalgo, Morelia, México

⁸Institute of Nuclear Physics Polish Academy of Sciences, PL-31342 IFJ-PAN, Krakow, Poland

⁹Instituto de Física, Universidad Nacional Autónoma de México, Ciudad de México, México

¹⁰Instituto Nacional de Astrofísica, Óptica y Electrónica, Puebla, México

¹¹Departamento de Física, Centro Universitario de Ciencias Exactas e Ingenierías, Universidad de

Guadalajara, Guadalajara, México

¹²Instituto de Astronomía, Universidad Nacional Autónoma de México, Ciudad de México, México

¹³Facultad de Ciencias Físico Matemáticas, Benemérita Universidad Autónoma de Puebla, Puebla, México

¹⁴Dept of Physics and Astronomy, University of New Mexico, Albuquerque, NM, USA

¹⁵Department of Physics and Astronomy, University of Utah, Salt Lake City, UT, USA

¹⁶Universidad Politécnica de Pachuca, Pachuca, Hgo, México

Key Points:

- We report on fairweather count rate bursts with 2ms duration following the impact of a large cosmic ray shower near a small scintillation detector at HAWC.
- Simulations show that the spectra and decay time can be produced by either hadronic interactions, or photoneutron reactions from gamma-rays.
- These results imply that downward TGFs could produce a similar delayed neutron signature in the soil near ground based detectors.

Corresponding author: Greg Bowers, gsbowers@lanl.gov

This article has been accepted for publication and undergone full peer review but has not been through the copyediting, typesetting, pagination and proofreading process, which may lead to differences between this version and the [Version of Record](#). Please cite this article as [doi: 10.1029/2020GL090033](https://doi.org/10.1029/2020GL090033).

This article is protected by copyright. All rights reserved.

Abstract

We report on anomalously long duration (2 ms) count rate bursts following the impact of cosmic ray showers near a 7.62 cm x 7.62 cm LaBr₃ scintillation detector at the High Altitude Water Cherenkov array in Mexico, previously described by Stenkin et al., 2001, and termed ‘neutron bursts’. The largest burst produced 198 counts within 2ms in our LaBr₃ detector. We simulate the neutron burst albedo flux (that is, secondary emissions from an extensive air shower core impacting the ground), and show that 1.) the characteristic spectra and count rates are well explained by neutron absorption in the ground and 2.) any cosmic ray secondary that produces neutrons, either through hadron inelastic collisions, or photoneutron production by gamma-rays, produces the same characteristic spectra. This implies that other natural phenomena that produce downward beams of gamma-rays, like Terrestrial gamma-ray flashes, should produce a similar ‘neutron burst’ signature from the photoneutron reactions occurring in the soil.

1 Cosmic Ray Showers

A cosmic ray-induced air shower is a particle cascade initiated at the top of the atmosphere by an incident primary cosmic ray whose angle with respect to zenith, θ , defines the shower axis. The cascading secondary particles form a pancake shaped front of particles normal to the shower axis that moves forward close to the speed of light. An air shower is typically composed of a hadronic core that continuously feeds electromagnetic and muonic particles laterally away from the shower axis as the shower travels downwards (Ziegler, 1998). For air showers initiated by cosmic rays near 10^{15} eV, the pancake can have a diameter, D , of 100 m, and a thickness, ΔL of 1 to 2 m by the time it reaches the ground (Gaisser et al., 2016). As a consequence of this geometry, all particles within the thickness of a small area on the pancake (order ΔL^2) will arrive at the ground within a very short time ($\Delta L/c \approx 3$ ns for a 1 m pancake thickness) as compared to the delay between the arrival of particles located at different ends of the pancake ($D/(c \sin \theta) \approx 500$ ns for a 100 m diameter pancake arriving along $\theta = 45^\circ$). By treating the pancake as a wavefront, large spatially distributed particle detector arrays (with dimensions on the order of the air shower footprint) like the High Altitude Water Cherenkov Array (HAWC) (Abeysekara et al., 2012), and the Large High Altitude Air Shower Observatory (LHAASO) (Bai et al., 2019) can infer the direction of the primary cosmic ray by tracking the time it takes the pancake to sweep across the array, and its energy by measuring the size and energy deposited by the footprint of the air shower that falls onto the array.

2 Neutron Bursts, or Cosmic Ray Shower Ground Interaction Albedo

From this simple picture, it is expected that a small, fast scintillator detector will observe the passage of an extended air shower as a single, piled-up pulse, or count (small means on the order of a few square meters, and fast means a scintillation decay time of 25-100 ns). However, an anomalously delayed phenomenon that produces many discrete counts observed up to several milliseconds following the passage of large air showers has been observed at neutron monitor observatories (Aushev et al., 1997; V. A. Antonova et al., 1999; V. P. Antonova et al., 2002) and other EAS arrays (Jędrzejczak et al., 2006; Shepetov et al., 2020). This delay is too long to be explained by statistical fluctuations in the longitudinal development of the air shower, which is on the order of 10s of nanoseconds (Agnetta et al., 1997), nor by spurious pulses produced by the PMT, such as afterpulsing, luminous reactions, and ionization of the residual gases, which can produce spurious pulses on the order of 10 ns - 10 μ s after primary pulses (Photonis, 2002; Abbasi et al., 2010). One hypothesis was that the delayed signal could be from the late arrival of non-relativistic (or ‘sub-luminal’) neutrons evaporated from air-nuclei following the passage of the air shower through the

86 atmosphere, termed ‘neutron thunder’, but this can only explain delays on the order of
 87 10s of microseconds, and cannot reproduce the observed exponential time distribution
 88 of delayed counts (Ambrosio et al., 1999). Stenkin et. al. termed these bursts of
 89 anomalously delayed counts ‘neutron bursts’, and showed that the delayed timescale
 90 and exponential distribution of their arrival times were consistent with evaporation
 91 neutrons created in the ground near the detector at the point of the cosmic ray shower
 92 core impact (Stenkin et al., 2001; Stenkin & Valdés-Galicia, 2002). The basic neutron
 93 burst mechanism is currently understood to be as follows:

- 94 1. a hadronic core of a cosmic ray shower produces many high energy evaporation
 95 neutrons in the ground near the detector;
- 96 2. these energetic neutrons thermalize and are absorbed over a timescale which
 97 depends on the composition of the ground;
- 98 3. these neutrons are captured in nuclei and produce high energy gamma-rays
 99 through (n, γ) reactions;
- 100 4. the anomalously delayed counts are due to these neutron capture gammas and
 101 their scattering products.

102 3 Neutron Burst observations at HAWC

103 Neutron bursts have recently been observed at HAWC at an altitude of 4.1 km
 104 in a 7.62x7.62 cm LaBr₃ scintillation detector attached to a spare data channel of
 105 the Broadband Interferometric Mapping and Polarization (BIMAP) sensor recently
 106 deployed to HAWC (Shao et al., 2018). BIMAP is an array of three broadband RF
 107 antennas, each consisting of two orthogonal linearly polarized dipoles with a bandwidth
 108 of 20-80 MHz. They are located north of the main HAWC water cherenkov detector
 109 (WCD) array shown in figure 1. The LaBr₃ scintillation detector is located in a small
 110 Pelican brand transport case sitting outside on the ground, and calibrated to bright
 111 spectral features of its internal radioactivity, namely the prominent 1436 keV gamma
 112 + 32 keV x-ray peak from the decay of ¹³⁸₅₇La.

113 The LaBr₃ detector is an 38S38 St. Gobain BrillanCe380, connected to an
 114 Ortec Scintipak supplying 800 V to the detector PMT. The base PMT output is
 115 sampled at 190 MSPS when the BIMAP system is triggered. BIMAP is programmed to
 116 trigger when either the RF power on any antenna exceeds a certain threshold, or when
 117 the integrated LaBr₃ PMT pulse exceeds a certain level. For each trigger, BIMAP
 118 captures 15 ms of data with 5 ms pre-trigger data. The fairweather background in the
 119 LaBr₃ at HAWC is ~ 0.45 counts/ms, and whose spectra is dominated by the typical
 120 intrinsic background spectra of LaBr₃ shown in figure 11 of (*Saint Gobain Technical*
 121 *Note*, 2019).

122 An example of the largest neutron burst observed between September 2017 and
 123 September 2019 is shown in figure 2. The large pulse at $t=0$ corresponds to a saturated
 124 pulse in our detector and is associated with the passage of the cosmic ray shower
 125 pancake shown in figure 1.

126 Following the recovery of this large PMT pulse, there is a series of 198 counts
 127 from 6 μ s after the initial rising edge of the saturated pulse out to 2 ms post-trigger.
 128 We subtract off the falling baseline of the saturated pulse using a median filter window,
 129 and show the integrated pulse-height spectrum off these 198 counts in figure 2b. There
 130 is a notable peak near 511 keV. The count rate of these pulses in figure 2c follows an
 131 exponential fall-off with an e-folding time constant of $500 \pm 50 \mu$ s, as shown in figure
 132 2c.

133 We estimate that the pulse height out of our PMT saturates for energy deposits
 134 larger than ~ 8 MeV. We observe many of these ‘saturated’ pulses within a given

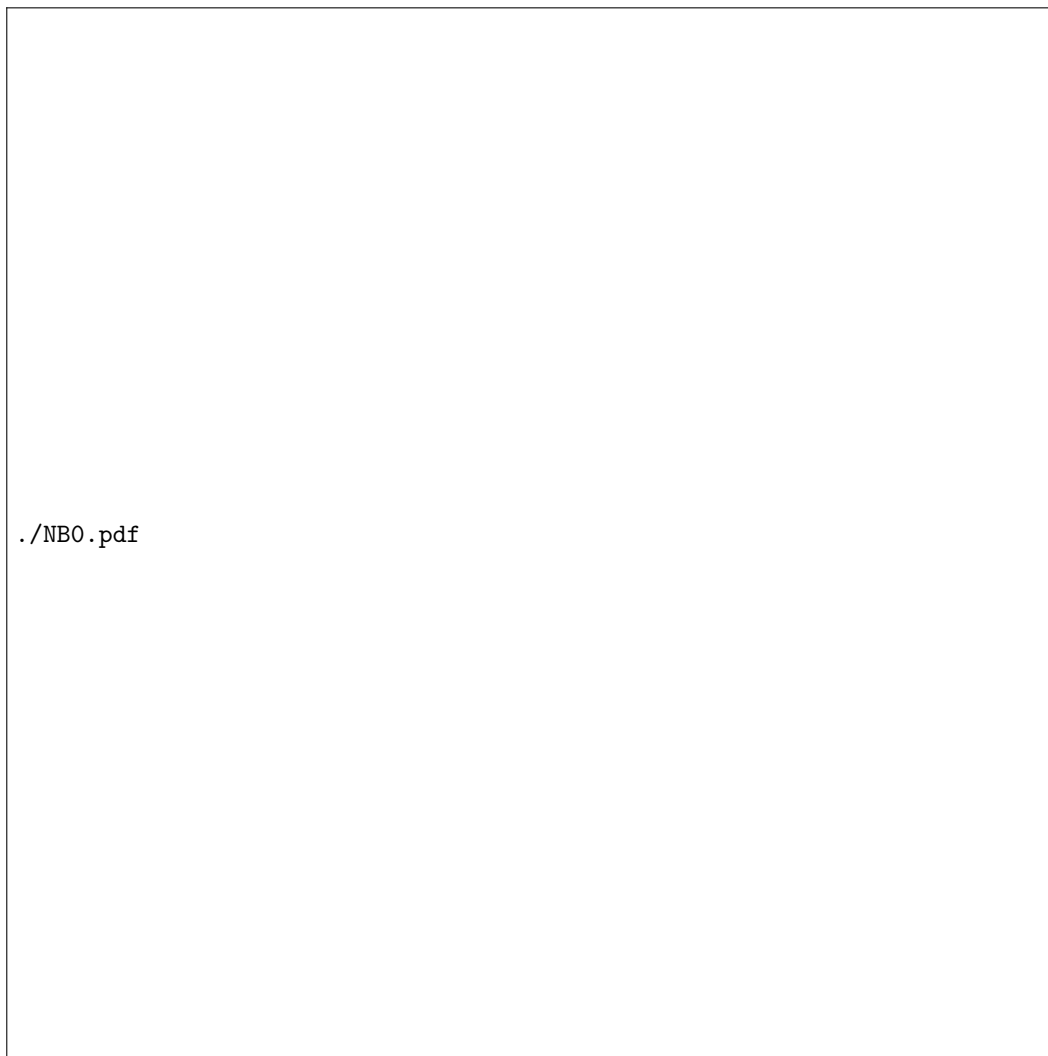


Figure 1. The 300 water cherenkov detectors (WCD) comprising the main HAWC array. Each WCD contains four PMTs. In this figure, the color indicates the arrival time at the tank of a cosmic-ray shower wavefront, and the size of the colored circle indicates roughly the energy deposited in the tank. The three antennas comprising the Broadband Interferometric Mapping and Polarization (BIMAP) instrument (colored diamonds) and the approximate location of the LaBr₃ detector (red cross) are indicated. The X-axis is along East-West, and Y-axis is North-South.

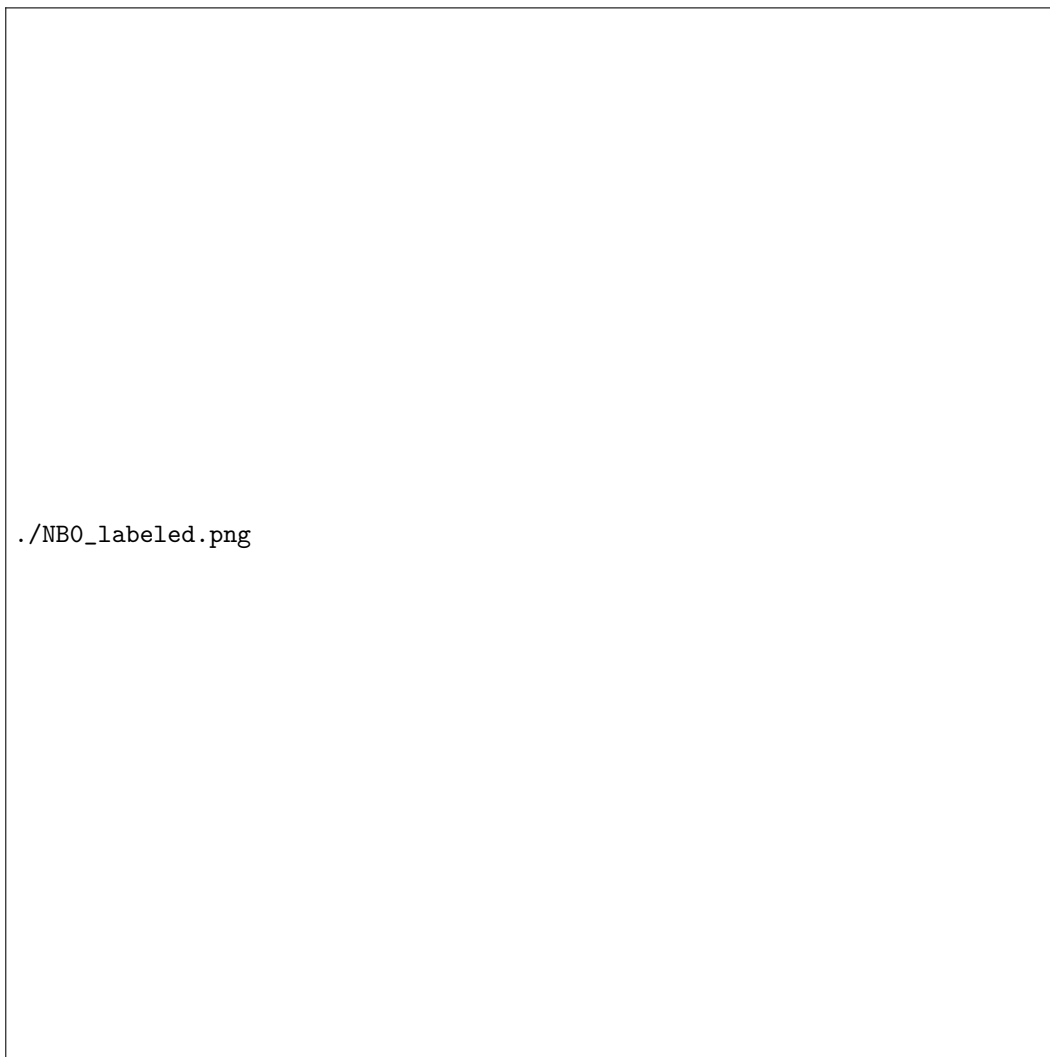


Figure 2. Neutron burst observed by a 7.62 cm x 7.62 cm LaBr₃ scintillation detector on 2018/08/13. (A) ~180 MHz sampled output from PMT coupled to the 7.62 cm x 7.62 cm LaBr₃ scintillation crystal. The large spike at $t=0$ corresponds to passage of cosmic ray shower (CRS). Subsequent pulses out to ≈ 2 ms correspond to particle interactions in the detector. (B) Energy spectrum of pulses from baseline-subtracted detector output waveform. There is notable peak near 511 keV. (C) Count rate of pulses after passage of cosmic ray shower at $t=0$. The Red line shows an exponential fit to the count rate, with a time constant of $500 \pm 50 \mu\text{s}$. (D, E) Detail of RF signals recorded by the BIMAP system during the passage of the CRS. (D) Interferometry can be used on the waveforms from antennas, A_0 , A_1 , and A_2 to provide a direction of the RF signal. (E) The signal from A_0 provides polarization (along East-West, or North-South). The black line shows the falling edge of the LaBr₃ PMT output, indicating the arrival of the CRS at the ground.

Time [UTC]	counts/2ms	τ [μ s]	BIMAP		HAWC		Precip [in]
			θ [$^\circ$]	ϕ [$^\circ$]	θ [$^\circ$]	ϕ [$^\circ$]	
2018-08-13/08:49:58.08860739*	198	500 ± 50	30	100	33	96.7	0.4 (0.4)
2018-08-05/06:36:28.60623834	79	536 ± 98	-	-	36.4	21.1	0.4 (0.8)
2018-10-06/07:12:54.97530532	40	925 ± 436	-	-	24.9	101.7	0.0 (0.1)
2018-07-29/08:42:03.15699945	45	754 ± 275	-	-	45.4	159.8	0.0 (0.2)
2018-06-05/07:36:25.40472688	45	731 ± 203	-	-	27.3	147.3	0.0 (0.0)
2018-12-23/11:36:08.79933614	33	1886 ± 1445	-	-	43.6	54.3	0.0 (0.0)
2019-05-16/18:19:49.49149813	56	583 ± 138	30	40	29	49	0.1 (0.5)

Table 1. The brightest neutron bursts observed at HAWC by a 7.62 cm x ϕ 7.62 cm LaBr₃ scintillation detector between Sept 2017 and Sept 2019. ‘Counts’ is the total number of counts within a 2 ms interval, >50 keV, recorded in the LaBr₃ detector, starting at 6 μ s after the impact of a large cosmic ray shower observed by HAWC. ‘ τ ’ is the time constant fit to the count rate using an exponential fall off. θ and ϕ are the zenith and azimuth angle of the cosmic ray shower reconstructed from HAWC and the Broadband Interferometric Mapping and Polarization Instrument (when possible). ‘Precip’ shows the recorded precipitation the day of and previous day (in parenthesis) as reported by <https://www.meteoblue.com/en/weather/historyclimate/weatherarchive/18.995N-97.308E>. *See figure 1 & 2.

135 day, likely the minimum ionizing energy deposits from typical background cosmic ray
136 muons, but they are typically not followed by any significant delayed counts after t=0.

137 From the timing of the pancake wavefront sweeping over the array, the direction
138 of this shower was determined to be from a zenith angle θ of 30 degrees, and an
139 azimuth angle ϕ of 100 degrees counter clockwise from east. Because the footprint
140 of this pancake exceeds the size of the HAWC array (as did all showers observed
141 coincident with the neutron bursts listed in table 1.), the primary energy could not be
142 determined (further work is needed to constrain the lower energy limit of these showers
143 using the array reconstruction), the shower’s impact location could not be determined,
144 and the nature of the air-shower (gamma-generated vs hadron-generated) could not
145 be determined.

146 Coincident with the arrival of the cosmic ray shower at the array, BIMAP de-
147 tected an impulsive, linearly polarized (along east-west) RF pulse, associated to a
148 source in the sky with the same zenith and azimuth as determined by HAWC for the
149 cosmic ray shower figure 2d,e. Large cosmic ray showers (with energy above 10^{16} eV)
150 are expected to produce detectable RF signals, with mainly east-west polarization due
151 to the deflection of the positrons and electrons in the Earth’s magnetic field and other
152 effects (Huege, 2016).

153 Neutron bursts at HAWC were discovered by searching the LaBr₃ records for
154 large count rate events (> 30 counts within 2 ms). In Table 1 we list the 7 brightest
155 neutron bursts observed at HAWC by the LaBr₃ scintillation detector between Sept
156 2017 and Sept 2019. For every instance where the LaBr₃ observed a large spike followed
157 by a significant number of delayed counts, HAWC observed a large cosmic ray shower
158 whose footprint exceeded the size of the array.

159 All of these events occurred during fair-weather days, meaning that there was no
160 nearby thunderstorm activity.

161 In addition to the 7 bright events discussed here, there was found to be a con-
 162 tinuum of ‘fainter’ events (meaning less than 30 counts within 2 ms observed in the
 163 LaBr₃), which will be the subject of future work.

164 4 Neutron burst spectra compared to simulated CRS Albedo Flux

165 For this work we simulate the albedo gamma-ray flux from a cosmic ray shower
 166 and compare to our LaBr₃ observations. In the first stage we use CORSIKA (Heck
 167 et al., 1998) (v.7.6400, QGSJET for high-energy hadrons, GHEISHA for low energy
 168 hadrons, and EGS4 for the electromagnetic component) to simulate the flux of air
 169 shower particles that arrive at 4.1 km from a 10¹⁷ eV cosmic-ray proton entering the
 170 top of the atmosphere at vertical incidence ($\theta = 0$), with a magnetic field set to the
 171 field value at the HAWC site, e.g. 27.717 μ T North and 29.907 μ T downwards. We
 172 choose 10¹⁷ eV TeV as the primary energy to be sufficiently large so as to produce a
 173 detectable RF signal (as was observed). We track the particle types (γ , e^\pm , n , p , μ^\pm , π^\pm ,
 174 etc), their momentum, and radial offset from shower nadir. For γ s, and e^\pm s, we track
 175 energies down to 10 MeV. For hadrons (n , p , π^\pm), CORSIKA only tracks energy down
 176 to 50 MeV. We assume all air shower particles arrive at the ground at time $t=0$. In
 177 the second stage, we use GEANT4 (Agostinelli et al., 2003; Allison et al., 2006, 2016)
 178 (v.10.04.p02, using FTFP_BERT_HP_LIV) to throw these secondary particles into a
 179 mass model of the ground, being SiO₂ with a density of 2 g/cm³, and record the flux of
 180 gamma-rays (their energy and radial offset from nadir) emitted from the surface of the
 181 ground starting from 6 μ s after shower impact. We term the gamma-rays produced by
 182 this process the gamma-ray albedo flux. We note that GEANT4 does not model particle
 183 interactions above 100 TeV. For this work, any secondary shower particles from the
 184 CORSIKA simulation above 100 TeV are simply thrown as a particle with energy 99.9
 185 TeV. The average and individual spectra of albedo gammas and their count rates within
 186 a 1 meter diameter of the shower impact from 10 simulations are shown in figure 3,
 187 and are compared to the 7 brightest neutron bursts observed at HAWC between 2017
 188 to 2019. This model simulation is consistent with recent observations by (Shepetov et
 189 al., 2020) who found that excess neutron flux typically required the impact of large
 190 showers ($E_0 > 10^{16}$ eV) within close proximity of the detectors ($r < 5 - 10$ m).

191 We note that there is qualitative agreement between the observed LaBr₃ spectra
 192 and the simulated gamma-ray albedo flux from a cosmic ray shower, notably the
 193 prominent peak at 511 keV. While we do not simulate the LaBr₃ detector response,
 194 assuming an effective area equal to the geometric area of the LaBr₃ crystal, $A_{\text{eff}} =$
 195 60cm², the expected number of counts from our simulated albedo flux, ϕ_γ , is $A_{\text{eff}}\phi_\gamma$,
 196 and is comparable in magnitude to the observed spectra (@ 500 keV, 8 counts observed
 197 vs 4.2 simulated). In addition, there is qualitatively good agreement between the
 198 observed LaBr₃ count rate time distribution and the simulated gamma-ray flux time
 199 distribution, namely, each exhibits a falling exponential distribution characterized by
 200 a similar e-folding time. As discussed in (Stenkin et al., 2001; Stenkin, Djappuev, &
 201 Valdés-Galicia, 2007; Stenkin, Volchenko, et al., 2007), this e-folding time is expected
 202 to be related to the rate of neutron absorption, which in soil can be calculated as
 203 $\tau_{\text{SiO}_2} = \lambda_{\text{abs}}/v_t$, where v_t is the thermal neutron speed ≈ 2200 m/s, and λ_{abs} is the
 204 mean free path for absorption. In pure soil with $\rho = 2$ g/cm³, $\lambda_{\text{abs}} \approx 2.5$ m, and
 205 $\tau_{\text{SiO}_2} \approx 1.1$ ms. This time constant can be reduced by decreasing the mean free path
 206 for neutron absorption, which can be done by either increasing the density of the soil,
 207 or adding water content. For pure soil with $\rho = 5$ g/cm³, the time constant becomes
 208 488 μ s (but this is an unreasonably high density for soil). For soil with $\rho = 2$ g/cm³
 209 and 6% water content by weight, the time constant is 661 μ s (figure 3d), consistent
 210 with an observed time constant of 500 μ s. In 1 we list the recorded precipitation on the
 211 day of and previous day of neutron burst observation, and note that there is generally

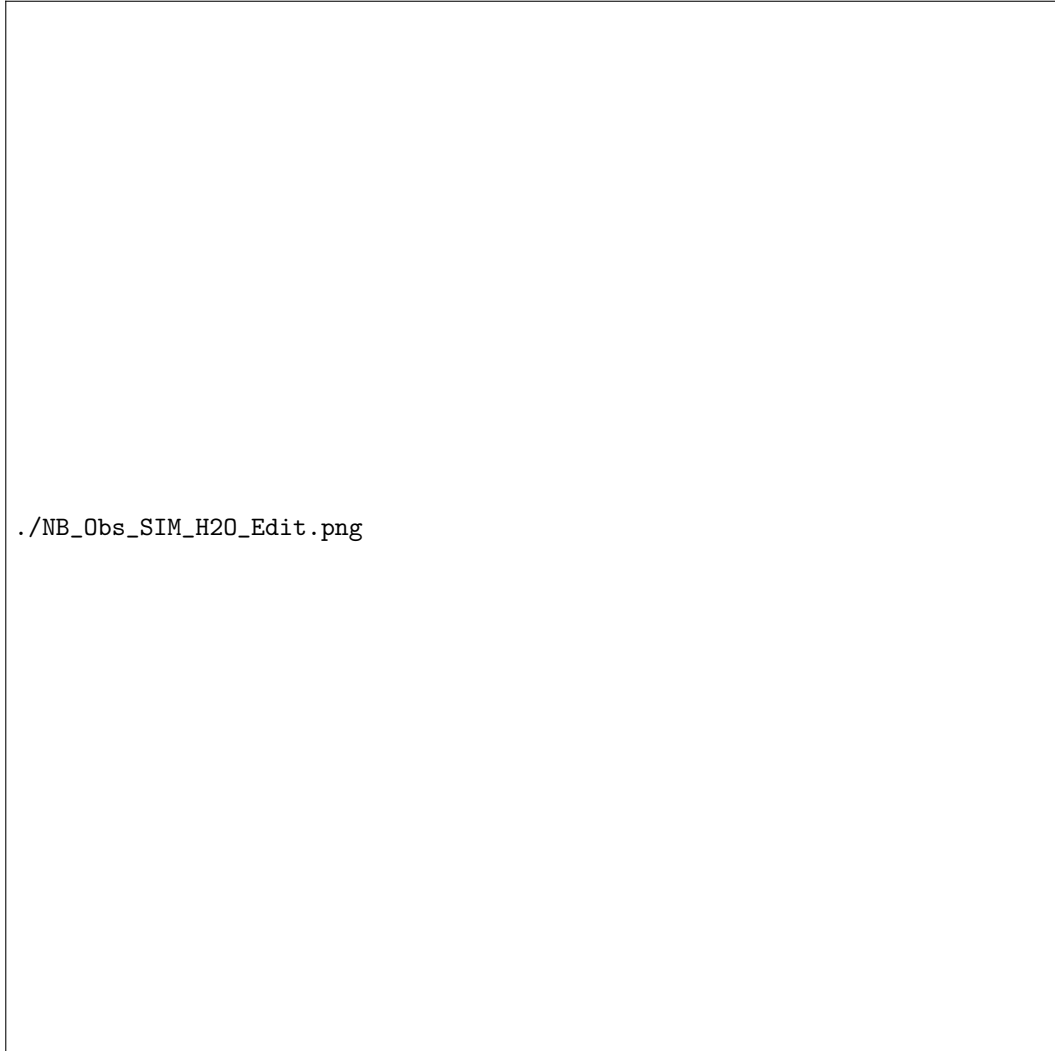


Figure 3. (A) Observed Spectra and (B) Count rate of the 7 brightest neutron bursts that occurred at HAWC between 2017 to 2019. Black histograms show brightest neutron burst event on 180813. Red histograms show averages of 6 next brightest events, shown individually by grey lines. (C) Simulated Spectra and (D) Count rates of albedo gammas (> 50 keV, and occurring $> 6 \mu\text{s}$ after CRS ground impact) resulting from the development of a 10^{17} eV proton air shower at 4.1 km input into a ground of SiO_2 . 5 individual runs are indicated by black lines, their average is indicated in red.



Figure 4. (Left) Spectra of secondaries in an air shower at 4.1 km produced from a $10^{17} eV$ vertically incident proton at the top of the atmosphere. Vertical dashed line indicates CORSIKA's 50 MeV cutoff for tracking hadrons. (Right) The average contribution of each air shower secondary species at 4.1 km to the flux of albedo gammas (> 50 keV, occurring $> 6 \mu s$ after CRS ground impact, within 0.5 m of nadir) from ten vertically incident 10^{17} eV proton air showers.

a trend of smaller time constants associated with more rain the day before, consistent with the model above.

5 Discussion

It is perhaps surprising that only 2 of the 7 strongest neutron burst events were accompanied by a detectable RF signature in BIMAP, as the diameter of the RF footprint for high signal amplitudes (associated with near-vertical showers) is on the order of 100-200 m, and for lower signal amplitudes (associated with zenith angles near 50°) is up to 1000 m (Huege, 2018). The separation between the LaBr₃ detector and the closest BIMAP antenna (A0) is 19m. It may be that the shower energy threshold for producing observable neutron bursts in our small scintillator is below the threshold

for detectable RF, or that there are different combinations of impact geometry that will produce observable neutron bursts and no RF, or vice versa.

The simulations we have presented are fairly rough (for example, it is undesirable that CORSIKA only tracks hadrons down to above 50 MeV (recent TGF simulation work by Ortega (Ortega, 2020) has used FLUKA to model hadrons down to 100 keV), we did not simulate the shower at the observed zenith angle for our brightest event, nor over a spectra of primary energies, and GEANT4 is not suited to handling particles above 100 TeV), but we can still make some significant fundamental observations from these results.

The prominent spectral feature in the observation and simulations near 0.5 MeV is a 511 keV positron-annihilation line. These positrons arise from pair production of high-energy gamma quanta produced in the neutron-capture (n, γ) reactions. For example, in the cascade of nuclear gamma-ray emissions resulting from the $^{28}\text{Si}(n, \gamma)^{29}\text{Si}$ reaction, the most likely emissions are 3.5 MeV and 4.9 MeV gammas, and the ratio of the cross sections for pair production and Compton scattering in soil at these energies is approximately 0.1. This means that 10% of n-cap gamma interactions in the soil will produce a positron that will annihilate to give a 511 keV gamma.

In figure 4, we show the total spectra of secondaries in the air shower at 4.1 km produced by a vertically incident 10^{17} eV proton in the atmosphere (figure 4a), and the contribution each secondary species makes to the total gamma-ray albedo flux (Figure 4b). Figure 4b shows that the characteristic gamma-ray albedo spectrum is largely independent of the incident secondary particle species into the ground. The reason is that the spectrum is due to neutrons, which can be produced through either hadronic interactions from hadrons, or photoneutron reactions from gammas. For our simulation, the most dominant contribution to the neutron burst spectra is from secondary gamma-rays, and as far as we know, this is the first time that photoneutron production in the ground has been considered in modeling neutron bursts, with previous work only considering hadronic interactions (Stenkin & Valdés-Galicia, 2002; Stenkin, Djappuev, & Valdés-Galicia, 2007).

6 Conclusions

- (1) We present the first spectrum of a cosmic ray neutron burst, observed at HAWC, and show that neutron burst spectrum and decay rates are consistent with reactions associated with thermal neutron absorption reactions in the ground.
- (2) From our rough simulations, we show that the characteristic neutron burst albedo spectra and count rate are independent of the secondary particle species impacting the ground, as long as the particle type is effective at making neutrons, either through direct hadronic interactions in the soil, or photoneutron production in the soil from gamma-rays through the (γ, n) reaction. This means that the signature of neutron bursts should be expected from any large cosmic ray shower that has a sufficiently large electromagnetic component, even ‘coreless’ showers (Stenkin, 2003) at lower altitudes.
- (3) A detectable RF signal with mainly east-west polarization was associated with the largest neutron burst observed, which produced 198 counts over 2 ms in our $7.62\text{x}7.62$ cm LaBr_3 scintillation detector, as well as a smaller burst, which produced 56 counts over the same time interval. RF signals associated with Cosmic Ray Showers were first observed in 1965 (Askar’yan, 1965), with many groups continuing these observations today (Ardouin et al., 2005; Fliescher & Pierre Auger Collaboration, 2012; Schellart et al., 2014; Scholten et al., 2016; Bezyazeev et al., 2015; Aab et al., 2016b, 2016a; Shao et al., 2018). This work highlights the likelihood that observations of strong cosmic ray RF signals may indicate the presence of nearby neutron bursts. This with conclusion 2

also implies that a combination of small radiation detectors and sensitive RF receivers (like BIMAP) used for terrestrial gamma-ray flash (TGF) observations may be able to detect and study the passage of high energy cosmic ray showers ($>10^{16}$ eV).

- (4) This work suggests that TGFs could produce a detectable ‘neutron burst’ if the TGF occurs near the ground. If detected, TGF-related neutron bursts may provide a temporally distinct, but similar neutron signature in detectors searching for thunderstorm neutrons (Babich, 2019). For example, a downward TGF produces 3 distinct detector signatures: 1.) The arrival of the TGF gammas, with a duration of $\approx 100 \mu\text{s}$ (Hare et al., 2016); 2.) The neutron afterglow, resulting from the arrival of sub-luminal photon neutrons produced by TGF gammas in the atmosphere, with a duration of ≈ 100 ms (Bowers et al., 2017); 3.) the positron glow from the radioactive decay of photon neutron products in the atmosphere, lasting several seconds (Rutjes et al., 2017; Enoto et al., 2017). A neutron burst resulting from the TGF gammas incident on ground near a TGF detector would have a duration of a few milliseconds, and have spectral characteristics similar to the TGF neutron afterglow.

Acknowledgments

We would like to thank Masashi Kamogawa for his support and discussion.

The data used to generate the figures is available at DOI:10.6084/m9.figshare.12746531.

We would like to acknowledge the Domestic Nuclear Detection Office under competitively awarded Contract No. IAA: HSHQDC-16-X-00088. The views and conclusions contained in this document are those of the authors and should not be interpreted as necessarily representing the official policies, either expressed or implied, of the U.S. Department of Homeland Security or the Government. This work was supported by Laboratory Directed Research and Development project 20170179ER in Los Alamos National Laboratory.

We acknowledge the support from: the US National Science Foundation (NSF) (AGS-1613028) the US Department of Energy Office of High-Energy Physics; the Laboratory Directed Research and Development (LDRD) program of Los Alamos National Laboratory; Consejo Nacional de Ciencia y Tecnología (CONACyT), México (grants 271051, 232656, 260378, 179588, 239762, 254964, 271737, 258865, 243290, 132197, 281653)(Cátedras 873, 1563, 341), Laboratorio Nacional HAWC de rayos gamma; L’OREAL Fellowship for Women in Science 2014; Red HAWC, México; DGAPA-UNAM (grants AG100317, IN111315, IN111716-3, IA102715, IN109916, IA102019, IN112218); VIEP-BUAP; PIFI 2012, 2013, PROFOCIE 2014, 2015; the University of Wisconsin Alumni Research Foundation; the Institute of Geophysics, Planetary Physics, and Signatures at Los Alamos National Laboratory; Polish Science Centre grant DEC-2014/13/B/ST9/945, DEC-2017/27/B/ST9/02272; Coordinación de la Investigación Científica de la Universidad Michoacana; Royal Society - Newton Advanced Fellowship 180385. Thanks to Scott Delay, Luciano Díaz and Eduardo Murrieta for technical support.

References

- Aab, A., Abreu, P., Aglietta, M., Ahn, E. J., Al Samarai, I., Albuquerque, I. F. M., ... Zuccarello, F. (2016a, Jun). Energy estimation of cosmic rays with the engineering radio array of the pierre auger observatory. *Phys. Rev. D*, *93*, 122005. Retrieved from <https://link.aps.org/doi/10.1103/PhysRevD.93.122005> doi: 10.1103/PhysRevD.93.122005

- 322 Aab, A., Abreu, P., Aglietta, M., Ahn, E. J., Al Samarai, I., Albuquerque,
 323 I. F. M., ... Zuccarello, F. (2016b, Jun). Measurement of the radiation
 324 energy in the radio signal of extensive air showers as a universal estima-
 325 tor of cosmic-ray energy. *Phys. Rev. Lett.*, *116*, 241101. Retrieved from
 326 <https://link.aps.org/doi/10.1103/PhysRevLett.116.241101> doi:
 327 10.1103/PhysRevLett.116.241101
- 328 Abbasi, R., Abdou, Y., Abu-Zayyad, T., Adams, J., Aguilar, J. A., Ahlers, M., ...
 329 IceCube Collaboration (2010, Jun). Calibration and characterization of the
 330 IceCube photomultiplier tube. *Nuclear Instruments and Methods in Physics
 331 Research A*, *618*(1-3), 139-152. doi: 10.1016/j.nima.2010.03.102
- 332 Abeyssekara, A. U., Aguilar, J. A., Aguilar, S., Alfaro, R., Almaraz, E., Álvarez,
 333 C., ... Zepeda, A. (2012, May). On the sensitivity of the HAWC obser-
 334 vatory to gamma-ray bursts. *Astroparticle Physics*, *35*(10), 641-650. doi:
 335 10.1016/j.astropartphys.2012.02.001
- 336 Agnetta, G., Ambrosio, M., Aramo, C., Barbarino, G. C., Beaman, J., Biondo,
 337 B., ... Watson, A. A. (1997, Mar). Time structure of the extensive
 338 air shower front. *Astroparticle Physics*, *6*(3-4), 301-312. doi: 10.1016/
 339 S0927-6505(96)00064-3
- 340 Agostinelli, S., Allison, J., Amako, K., Apostolakis, J., Araujo, H., Arce, P., ...
 341 GEANT4 Collaboration (2003, July). GEANT4 - a simulation toolkit. *Nu-
 342 clear Instruments and Methods in Physics Research A*, *506*, 250-303. doi:
 343 10.1016/S0168-9002(03)01368-8
- 344 Allison, J., Amako, K., Apostolakis, J., Araujo, H., Dubois, P. A., Asai, M., ...
 345 Yoshida, H. (2006, February). Geant4 developments and applications. *IEEE
 346 Transactions on Nuclear Science*, *53*, 270-278. doi: 10.1109/TNS.2006.869826
- 347 Allison, J., Amako, K., Apostolakis, J., Arce, P., Asai, M., Aso, T., ... Yoshida,
 348 H. (2016, November). Recent developments in GEANT4. *Nuclear
 349 Instruments and Methods in Physics Research A*, *835*, 186-225. doi:
 350 10.1016/j.nima.2016.06.125
- 351 Ambrosio, M., Chubenko, A. P., Erlykin, A. D., & Wolfendale, A. W. (1999, Mar).
 352 Thunderstorm model of the temporal EAS disc structure. *Nuclear Physics B
 353 Proceedings Supplements*, *75*(1-2), 336-339. doi: 10.1016/S0920-5632(99)00284-
 354 4
- 355 Antonova, V. A., Chubenko, A. P., Kokobaev, M. M., Shepetov, A. L., Vildanova,
 356 L. A., & Zhdanov, G. B. (1999, Mar). Phenomenon of the anomalous delay of
 357 hadronic and electronic components of EAS. *Nuclear Physics B Proceedings
 358 Supplements*, *75*(1-2), 333-335. doi: 10.1016/S0920-5632(99)00283-2
- 359 Antonova, V. P., Chubenko, A. P., Kryukov, S. V., Nesterova, N. M., Shepetov,
 360 A. L., Piskal, V. V., ... Zhdanov, G. B. (2002, Feb). Anomalous time struc-
 361 ture of extensive air shower particle flows in the knee region of primary cosmic
 362 ray spectrum. *Journal of Physics G Nuclear Physics*, *28*(2), 251-266. doi:
 363 10.1088/0954-3899/28/2/306
- 364 Ardouin, D., Belltoile, A., Charrier, D., Dallier, R., Denis, L., Eschstruth, P.,
 365 ... Ravel, O. (2005). Radio-detection signature of high-energy cos-
 366 mic rays by the codalema experiment. *Nuclear Instruments and Meth-
 367 ods in Physics Research Section A: Accelerators, Spectrometers, Detectors
 368 and Associated Equipment*, *555*(1), 148-163. Retrieved from [https://
 369 www.sciencedirect.com/science/article/pii/S0168900205017468](https://www.sciencedirect.com/science/article/pii/S0168900205017468) doi:
 370 <https://doi.org/10.1016/j.nima.2005.08.096>
- 371 Askar'yan, G. A. (1965, September). Coherent Radio Emission from Cosmic Show-
 372 ers in Air and in Dense Media. *Soviet Journal of Experimental and Theoretical
 373 Physics*, *21*, 658.
- 374 Aushev, V. M., Zhdanov, G. B., Kokobaev, M. M., Piskal, V. V., Romakhina, N. S.,
 375 Chubenko, A. P., & Shchepetov, A. L. (1997). Multiplicity spectrum of
 376 the NM-64 Tien Shan neutron supermonitor and energy spectrum of the

- 377 hadron component at mountains. *Bulletin of the Russian Academy of Sci-*
 378 *ences, Physics, 61*, 381-384.
- 379 Babich, L. P. (2019). Thunderstorm neutrons. *UFN, 189*(10), 1044-1069. Retrieved
 380 from [https://doi.org/10.1142/S021773230301105://doi.org/10.3367/](https://doi.org/10.1142/S021773230301105://doi.org/10.3367/UFNr.2018.12.038501)
 381 [UFNr.2018.12.038501](https://doi.org/10.1142/S021773230301105://doi.org/10.3367/UFNr.2018.12.038501) doi: 10.3367/UFNr.2018.12.038501
- 382 Bai, X., Bi, B. Y., Bi, X. J., Cao, Z., Chen, S. Z., Chen, Y., ... Zhu, H. (2019,
 383 May). The Large High Altitude Air Shower Observatory (LHAASO) Science
 384 White Paper. *arXiv e-prints*, arXiv:1905.02773.
- 385 Bezyazeev, P., Budnev, N., Gress, O., Haungs, A., Hiller, R., Huege, T., ...
 386 Zagorodnikov, A. (2015). Measurement of cosmic-ray air showers with
 387 the tunka radio extension (tunka-rx). *Nuclear Instruments and Meth-*
 388 *ods in Physics Research Section A: Accelerators, Spectrometers, Detec-*
 389 *tors and Associated Equipment, 802*, 89-96. Retrieved from [https://](https://www.sciencedirect.com/science/article/pii/S0168900215010256)
 390 www.sciencedirect.com/science/article/pii/S0168900215010256 doi:
 391 <https://doi.org/10.1016/j.nima.2015.08.061>
- 392 Bowers, G. S., Smith, D. M., Martinez-McKinney, G. F., Kamogawa, M., Cummer,
 393 S. A., Dwyer, J. R., ... Kawasaki, Z. (2017). Gamma ray signatures of neu-
 394 trons from a terrestrial gamma ray flash. *Geophysical Research Letters, 44*(19),
 395 10,063-10,070. Retrieved from [https://agupubs.onlinelibrary.wiley.com/](https://agupubs.onlinelibrary.wiley.com/doi/abs/10.1002/2017GL075071)
 396 [doi/abs/10.1002/2017GL075071](https://agupubs.onlinelibrary.wiley.com/doi/abs/10.1002/2017GL075071) doi: 10.1002/2017GL075071
- 397 Enoto, T., Wada, Y., Furuta, Y., Nakazawa, K., Yuasa, T., Okuda, K., ... Tsuchiya,
 398 H. (2017, November). Photonuclear Reactions in Lightning Discovered from
 399 Detection of Positrons and Neutrons. *arXiv e-prints*, arXiv:1711.08044.
- 400 Fliescher, S., & Pierre Auger Collaboration. (2012, January). Radio detection of
 401 cosmic ray induced air showers at the Pierre Auger Observatory. *Nuclear In-*
 402 *struments and Methods in Physics Research A, 662*, S124-S129. doi: 10.1016/j.
 403 [nima.2010.11.045](https://doi.org/10.1016/j.nima.2010.11.045)
- 404 Gaisser, T. K., Engel, R., & Resconi, E. (2016). *Cosmic Rays and Particle Physics*.
- 405 Hare, B. M., Uman, M. A., Dwyer, J. R., Jordan, D. M., Biggerstaff, M. I., Caicedo,
 406 J. A., ... Bozarth, A. (2016). Ground-level observation of a terrestrial
 407 gamma ray flash initiated by a triggered lightning. *Journal of Geophysi-*
 408 *cal Research: Atmospheres, 121*(11), 6511-6533. Retrieved from [https://](https://agupubs.onlinelibrary.wiley.com/doi/abs/10.1002/2015JD024426)
 409 agupubs.onlinelibrary.wiley.com/doi/abs/10.1002/2015JD024426 doi:
 410 [10.1002/2015JD024426](https://doi.org/10.1002/2015JD024426)
- 411 Heck, D., Knapp, J., Capdevielle, J. N., Schatz, G., & Thouw, T. (1998). *COR-*
 412 *SIKA: a Monte Carlo code to simulate extensive air showers*.
- 413 Huege, T. (2016). Radio detection of cosmic ray air showers in the digital era.
 414 *Physics Reports, 620*, 1 - 52. Retrieved from [http://www.sciencedirect](http://www.sciencedirect.com/science/article/pii/S0370157316000636)
 415 [.com/science/article/pii/S0370157316000636](http://www.sciencedirect.com/science/article/pii/S0370157316000636) (Radio detection of
 416 cosmic ray air showers in the digital era) doi: [https://doi.org/10.1016/](https://doi.org/10.1016/j.physrep.2016.02.001)
 417 [j.physrep.2016.02.001](https://doi.org/10.1016/j.physrep.2016.02.001)
- 418 Huege, T. (2018). Radio detection of cosmic rays achievements and future poten-
 419 tial. In *Proceedings of 2016 international conference on ultra-high energy cos-*
 420 *mic rays (uhec2016)*. Retrieved from [https://journals.jps.jp/doi/abs/10](https://journals.jps.jp/doi/abs/10.7566/JPSCP.19.011031)
 421 [.7566/JPSCP.19.011031](https://journals.jps.jp/doi/abs/10.7566/JPSCP.19.011031) doi: 10.7566/JPSCP.19.011031
- 422 Jędrzejczak, K., Karczmarczyk, J., Kasztelan, M., Petrochenkov, S. A., Polański, A.,
 423 Swarzyński, J., ... Wibig, T. (2006, Jan). Registration of neutrons within 2
 424 milliseconds after EAS impact. *Nuclear Physics B Proceedings Supplements,*
 425 *151*, 329-332. doi: 10.1016/j.nuclphysbps.2005.07.050
- 426 Ortega, P. G. (2020). Isotope production in thunderstorms. *Journal of At-*
 427 *mospheric and Solar-Terrestrial Physics, 208*, 105349. Retrieved from
 428 <http://www.sciencedirect.com/science/article/pii/S1364682620301620>
 429 doi: <https://doi.org/10.1016/j.jastp.2020.105349>
- 430 Photonis. (2002, Sep). *Photomultiplier Tubes Principles and Applications* (Tech.
 431 Rep.).

- 432 Rutjes, C., Diniz, G., Ferreira, I. S., & Ebert, U. (2017, October). TGF Afterglows:
 433 A New Radiation Mechanism From Thunderstorms. *Geophysical Research Let-*
 434 *ters*, *44*(20), 10,702-10,712. doi: 10.1002/2017GL075552
- 435 *Saint gobain technical note* (Tech. Rep.). (2019, April). Saint Gobain Crystals.
- 436 Schellart, P., Buitink, S., Corstanje, A., Enriquez, J. E., Falcke, H., Hörandel, J. R.,
 437 ... Trinh, T. N. G. (2014, October). Polarized radio emission from extensive
 438 air showers measured with LOFAR. *Journal of Cosmology and Astroparticle*
 439 *Physics*, *2014*(10), 014. doi: 10.1088/1475-7516/2014/10/014
- 440 Scholten, O., Trinh, T. N. G., Bonardi, A., Buitink, S., Correa, P., Corstanje, A., ...
 441 Winchen, T. (2016, November). Measurement of the circular polarization in
 442 radio emission from extensive air showers confirms emission mechanisms. *Phys-*
 443 *ical Review Letters D*, *94*(10), 103010. doi: 10.1103/PhysRevD.94.103010
- 444 Shao, X.-M., Ho, C., Caffrey, M., Graham, P., Haynes, B., Bowers, G., ... Rassoul,
 445 H. (2018). Broadband rf interferometric mapping and polarization (bimap)
 446 observations of lightning discharges: Revealing new physics insights into break-
 447 down processes. *Journal of Geophysical Research: Atmospheres*, *123*(18),
 448 10,326-10,340. Retrieved from [https://agupubs.onlinelibrary.wiley.com/](https://agupubs.onlinelibrary.wiley.com/doi/abs/10.1029/2018JD029096)
 449 [doi/abs/10.1029/2018JD029096](https://agupubs.onlinelibrary.wiley.com/doi/abs/10.1029/2018JD029096) doi: 10.1029/2018JD029096
- 450 Shepetov, A., Chubenko, A., Iskhakov, B., Kryakunova, O., Kalikulov, O., Mam-
 451 ina, S., ... et al. (2020, Jan). Measurements of the low-energy neutron and
 452 gamma ray accompaniment of extensive air showers in the knee region of pri-
 453 mary cosmic ray spectrum. *The European Physical Journal Plus*, *135*(1).
 454 Retrieved from <http://dx.doi.org/10.1140/epjp/s13360-019-00092-1>
 455 doi: 10.1140/epjp/s13360-019-00092-1
- 456 Stenkin, Y. V. (2003). Does the "knee" in primary cosmic ray spectrum exist? *Mod-*
 457 *ern Physics Letters A*, *18*(18), 1225-1234. Retrieved from [https://doi.org/](https://doi.org/10.1142/S0217732303011058)
 458 [10.1142/S0217732303011058](https://doi.org/10.1142/S0217732303011058) doi: 10.1142/S0217732303011058
- 459 Stenkin, Y. V., Djappuev, D. D., & Valdés-Galicia, J. F. (2007, Jun). Neutrons in
 460 extensive air showers. *Physics of Atomic Nuclei*, *70*(6), 1088-1099. doi: 10
 461 .1134/S1063778807060117
- 462 Stenkin, Y. V., & Valdés-Galicia, J. F. (2002, Jan). On the Neutron Bursts
 463 Origin. *Modern Physics Letters A*, *17*(26), 1745-1751. doi: 10.1142/
 464 S0217732302008137
- 465 Stenkin, Y. V., Valdés-Galicia, J. F., Hurtado, A., & Musalem, O. (2001, Nov).
 466 Study of "neutron bursts" with Mexico City neutron monitor. *Astroparticle*
 467 *Physics*, *16*(2), 157-168. doi: 10.1016/S0927-6505(01)00101-3
- 468 Stenkin, Y. V., Volchenko, V. I., Dzhappuev, D. D., Kudzhaev, A. U., & Mikhailova,
 469 O. I. (2007, Apr). Neutrons in extensive air showers. *Bulletin of the*
 470 *Russian Academy of Sciences, Physics*, *71*(4), 541-544. doi: 10.3103/
 471 S1062873807040314
- 472 Ziegler, J. F. (1998, Jan). Terrestrial cosmic ray intensities. *IBM Journal of Re-*
 473 *search and Development*, *42*(1), 117-139.